
Quantification of airborne particulate matter and trace elements deposition on Hedera helix and Senecio cineraria leaves

[Anabel Saran](#)*, Mariano Javier Mendez, [Diego Gabriel Much](#), Valeria Imperato, [Sofie Thijs](#), [Jaco Vangronsveld](#), Luciano Jose Merini

Posted Date: 17 July 2024

doi: 10.20944/preprints202407.1414.v1

Keywords: particulate matter; air pollution; trace elements; bio-monitors; plants.



Preprints.org is a free multidiscipline platform providing preprint service that is dedicated to making early versions of research outputs permanently available and citable. Preprints posted at Preprints.org appear in Web of Science, Crossref, Google Scholar, Scilit, Europe PMC.

Copyright: This is an open access article distributed under the Creative Commons Attribution License which permits unrestricted use, distribution, and reproduction in any medium, provided the original work is properly cited.

Article

Quantification of Airborne Particulate Matter and Trace Elements Deposition on *Hedera helix* and *Senecio cineraria* Leaves

Anabel Saran ^{1,*}, Mariano Mendez ², Diego Much ¹, Valeria Imperato ³, Sofie Thijs ³, Jaco Vangronsveld ^{3,4} and Luciano Merini ¹

¹ CONICET, Agency of Scientific Investigation, La Pampa, Argentina; saran.anabel@gmail.com; diego.much@live.com.ar; lucianomerini@yahoo.com.ar

² CONICET, Universidad Nacional de La Pampa, Facultad de Agronomía, Argentina; marianomendez@hotmail.com

³ Environmental Biology, Centre for Environmental Sciences, Hasselt University, Diepenbeek, Belgium; vale.imperato@gmail.com; sofie.thijs@uhasselt.be

⁴ Department of Plant Physiology and Biophysics, Institute of Biological Sciences, Maria Curie Skłodowska University, Lublin, Poland; jaco.vangronsveld@uhasselt.be

* Correspondence: saran.anabel@gmail.com

Abstract: Both, in developed and developing countries, atmospheric pollution with particulate matter (PM) remains an important issue. Despite the health effects of poor air quality, studies on air pollution are often limited by the high costs of continuous monitoring and the need of extensive sampling. Furthermore, these particles are often enriched in potentially toxic trace elements and organics pollutants. This study evaluates both, the composition of atmospheric dust accumulated during a certain time-span on leaves of *Hedera helix* and *Senecio cineraria*, as well as the potential to use them as bio-monitors. The test plants were positioned nearby automatic air quality monitoring stations at four different sites with respectively high, moderate and low traffic intensity. Gravimetric deposition of PM₁₀ and PM_{2.5} on leaves was consistent with data recorded by the monitoring stations and related to the weather conditions reported by Argentina's National Meteorological service. To determine the presence of trace elements enriching the PM deposited on leaves, two analytical techniques were applied, XRF (not destructive) and ICP (destructive). The results indicated that only in the unpaved street location (site 2), PM₁₀ and PM_{2.5} concentrations in the air exceeded WHO guidelines. However, several trace elements were found enriching PM deposited on leaves from all sites. Predominantly, increased concentrations of Cd, Cu, Ti, Mn, Zn and Fe were found, which were associated to construction, traffic and unpaved street sources. Furthermore, based on its high capability to sequester PM and trace elements *Senecio cineraria* can be take into consideration to be adopted as a bio-monitor or even for PM mitigation.

Keywords: particulate matter; air pollution; trace elements; bio-monitors; plants

1. Introduction

According to the report of the European Environment Agency (EEA, 2017), air pollution is a major environmental and social problem, which leads to multiple challenges in terms of management and mitigation. Effective action to reduce the impacts of air pollution requires a good understanding of how pollutants are transported and transformed in the atmosphere, and how they affect humans, ecosystems, the climate and, subsequently, the society and economy [1]. Suspended particulate matter (PM) is an important atmospheric pollutant with severe public health effects, particularly in urban areas which are heavily affected by emissions from vehicles, industry, and other sources of air pollution [2]. The correlation between emissions and pollution levels differs depending on the city

and even part of a city, where infrastructure and urban planning determine the emission pattern while meteorology and topography determine dispersion and transformation [3].

Inhalable PM refers to particles with a diameter less than 10 μm . These particles have a complex composition, including organic constituents, inorganic salts, and trace elements [4]. Different studies have associated PM10 with severe respiratory diseases, such as asthma [5], lung cancer [6], and chronic obstructive pulmonary disease [7], as well as with cardiovascular diseases such as stroke, deep vein thrombosis, coronary events, myocardial infarctions and atherosclerosis [8]. Between 1990 and 2019, worldwide deaths due to air pollution enhanced by 2.62%. Furthermore, over 90% of the global population resides in areas that are not reach the air quality standards established by the WHO (2021) [2].

Despite the impact of air quality on health, studies of air pollution are often restricted by the high costs of monitoring instruments and the too limited scale of sampling. Drawbacks of the conventional monitoring equipment is the high price, large size, heavy weight and energy consumption [9]. For these reasons, bio-monitoring, that is the use of plants or lichens to estimate air quality, has been proposed as a cost-effective and environmentally friendly approach which can be an alternative for physical and chemical analytical methods of air pollution monitoring [10]. In this way, plants got introduced as bio-monitors of trace elements accumulation due to their efficiency for trapping particulate matter [11]. Air pollutants can be bounded in and on the cuticula and, eventually, taken up by plants via stomata, or indirectly by uptake via roots after deposition of the air pollutants on the soil [12]. After penetration, the particles clog the stomata and decrease the foliar pH due to the presence of sulphate (SO_4^{2-}) and nitrate (NO_3^-) ions in the dust [13]. Atmospheric dust deposition on leaves is mainly influenced by the plant species (evergreen or deciduous, composition and thickness of wax layer) and the specific structure of their leaves (e.g. leaf size, shape, roughness, presence of trichomes), as well as the meteorological conditions (air humidity, rainfall, wind) and source-specific particle features (e.g. particle size distribution) [14]. In this context, improvement of green spaces or shelter belts by planting suitable and tolerant species, selected for the specific area, can catch air pollutants and mitigate the pollution levels.

This study aimed to assess the levels of air pollution in sites with high, moderate and low traffic intensity, relating bio-monitors with automatic monitors data, as well as to assess the usefulness of destructive and non-destructive analytical techniques for the quantification of trace elements using outdoor exposed *Hedera helix* and *Senecio cineraria* plants.

2. Results

2.1. Daily Meteorological Conditions and Air Quality Monitoring Stations

The highest temperature (higher than 30 $^{\circ}\text{C}$) was recorded in the summer season in January (13/01/2022) (Figure 1). Relatively strong winds appeared between 25/10/2021 and 10/11/2021, being 20 times stronger than the average for the rest of the recorded days. Humidity fluctuated between 31.75% and 96.46%, being the last one consistent with the peak precipitation recorded (62.4 ml/m²; 3/12/2021).

The monthly mean PM concentrations recorded by automatic monitors are presented in Figure 2. Site 2 (moderate car traffic and unpaved street) is the only site exceeding the PM2.5 threshold recommended by WHO (2021). September and October (spring season) were the months with the highest PM2.5 concentrations recorded. Also, monthly mean PM10 concentrations (Figure 2) recorded at Site 2 exceeded the WHO threshold, as well as at Site 3 (moderate car traffic), however the mean concentrations recorded in this site were significantly lower than that recorded at Site 2, showing that the biggest contribution of PM10 mainly originated from the unpaved street. In Figure S4, daily average concentrations recorded for PM10 and PM2.5 at each site are presented.

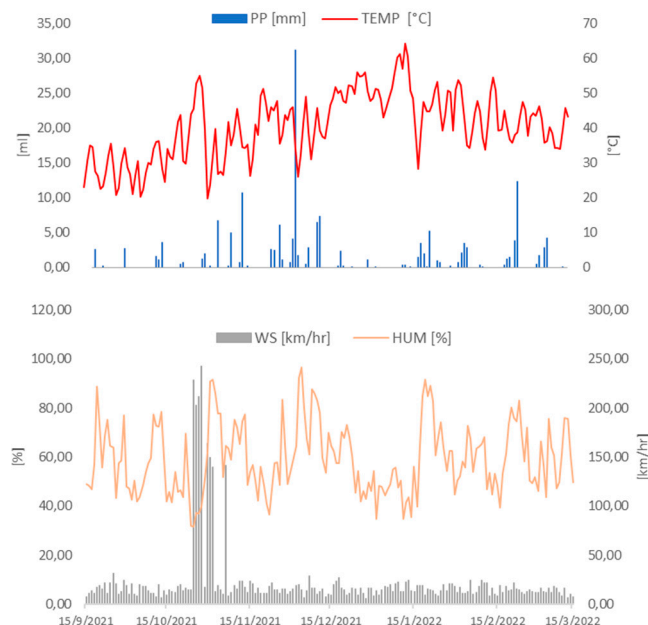


Figure 1. Measurements from an automatic weather station from the National Weather Service of Argentina at Santa Rosa Aero station. Humidity (orange line), wind speed (grey bars), temperature (red line) and precipitation recorded (blue bars) between 15/09/2021 and 15/03/2022.

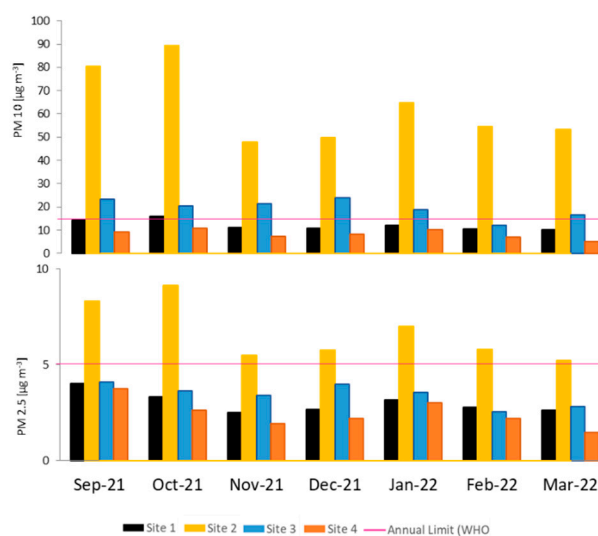


Figure 2. Average concentrations of PM 10 and PM 2.5 recorded monthly at each site (n=5). Pink line represents the WHO annual limit recommended (PM 10= 15 $\mu\text{g m}^{-3}$; PM2.5= 5 $\mu\text{g m}^{-3}$).

Spearman correlation matrix (Figure 3) showed a positive correlation ($p < 0.05$) between temperature and PM10 and PM2.5 for sites 3 and 4. A negative correlation ($p < 0.05$) was observed between humidity and PM10 across all sites. While, a slight negative correlation ($p < 0.05$) between humidity and PM2.5 was seen for sites 2 and 3. Only at site 4 a positive correlation ($p < 0.05$) (Figure 3) was identified for PM10 and wind speed. Concerning precipitation, a negative correlation ($p < 0.05$) was observed across all sites for PM10, whereas this correlation is evident only at sites 2 and 3 when considering PM2.5.

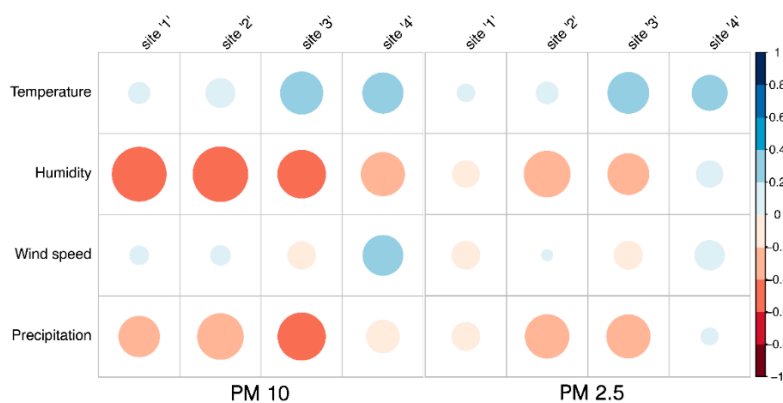


Figure 3. Spearman correlation matrix, pairwise relationships between meteorological variables and PM concentrations recorded by monitors located at the four sites. Circle sizes dynamically adjust based on the magnitude of correlation and the color gradient indicate the strength and direction of correlations, from negative (red) to positive (blue).

2.2. Gravimetric Quantification of Particulate Matter Deposited on Leaves

Table 1 shows the mean concentrations, and standard errors, of PM10 and PM2.5 deposited on leaves of *Hedera helix* and *Senecio cineraria*. ANOVA indicates significant differences in the amounts of PM10 quantified from the leaf surfaces of *Hedera helix* and *Senecio cineraria* ($p > 0.05$). *Senecio cineraria* sequestered between 2 to 8 times more PM10 per cm^2 than *Hedera helix*. This can be explained by the micromorphology of *Senecio cineraria* leaves (Figure S3), which appeared more rugged than *Hedera* leaves. We also found significant differences in PM2.5 deposited at site 3 ($p > 0.05$), where both species sequestered the highest amounts of PM2.5 (*Hedera*: $965 \mu\text{g}\cdot\text{cm}^{-2}$; *Senecio*: $2450 \mu\text{g}\cdot\text{cm}^{-2}$). For both species, significant increases in PM10 and PM2.5 were observed after 3 months at site 3 ($p > 0.05$) and after 6 months at site 4 ($p > 0.05$). At sites 1 and 2, species behaved differently. At site 1, *Hedera* didn't show any significant accumulation of PM10 and PM2.5; in contrast, for *Senecio* the amount of PM10 increased significantly ($p > 0.05$) after 3 months while the amount of PM2.5 decreased. After 6 months at site 2, significant increases were observed for PM2.5 on *Hedera* and for PM10 on *Senecio*.

Table 1. PM10 and PM2.5 ($\mu\text{g}\cdot\text{cm}^{-2}$) sequestered on leaf surface.

Plant	Time	Site 1		Site 2		Site 3		Site 4	
		PM10	PM2.5	PM10	PM2.5	PM10	PM2.5	PM10	PM2.5
<i>Hedera helix</i>	0m	485±96 ^a	681±125 ^a	930±175 ^a	115±44 ^a	60±26 ^a	30±23 ^a	151±51 ^a	109±90 ^a
	3m	341±83 ^a	552±588 ^a	699±274 ^{ab}	670±577 ^{ab}	946±312 ^b	965±343 ^b	175±81 ^a	215±90 ^a
	6m	412±43 ^a	505±465 ^a	501±330 ^{ab}	682±198 ^b	697±92 ^b	1016±682 ^b	752±435 ^b	601±359 ^b
<i>Senecio cineraria</i>	0m	429±176 ^a	691±235 ^a	260±153 ^a	231±159 ^a	55±26 ^a	43±50 ^a	234±138 ^a	152±48 ^a
	3m	2893±3634 ^{ab}	140±54 ^b	1686±2174 ^{ab}	344±159 ^{ab}	2450±264 ^b	2450±343 ^c	158±83 ^a	231±114 ^a
	6m	2800±884 ^b	132±44 ^b	649±242 ^b	383±55 ^{ab}	1056±538 ^b	1047±582 ^b	623±329 ^b	548±94 ^b

Values are mean \pm S.E. (n = 5). Values in a column followed by the same letter are not significantly different at $p \leq 0.05$ by ANOVA and Tukey test.

2.3. Leaf Surface Elemental Composition: XRF and ICP

The means (n=5) of the XRF spectra of *Hedera helix* and *Senecio cineraria* are presented in Figures 4 and 5 respectively. Supporting information Table S1 presents the mean element distributions and deviations obtained. K and L x-ray emission lines were preset to perform the quantification. Initially, an assessment was made of the elements present on the nonexposed clean leaves (0 months) (gray spectra in Figures 4 and 5). The elements Al, Si, P, S, K, Ca, Mn and Fe, were present in all non-exposed clean leaves for both *Hedera helix* and *Senecio cineraria* plants, of which Si, K and Ca were the

most abundant elements. After 3 and 6 months, the predominant elements determined by XRF included Ti, Zn and Fe. The Ti mean element distribution was similar for *Hedera* and *Senecio* located at site 2. Also, *Senecio* plants located at site 1 showed Ti accumulation. Zn accumulation was observed in *Hedera* plants located at site 2 and *Cineraria* plants located at site 1. Fe found in *Senecio* leaves (normalized weight %) was more than three times higher than the found on *Hedera*. However, the observed variabilities between leaves from the same species and exposure time were larger than expected (Table S1).

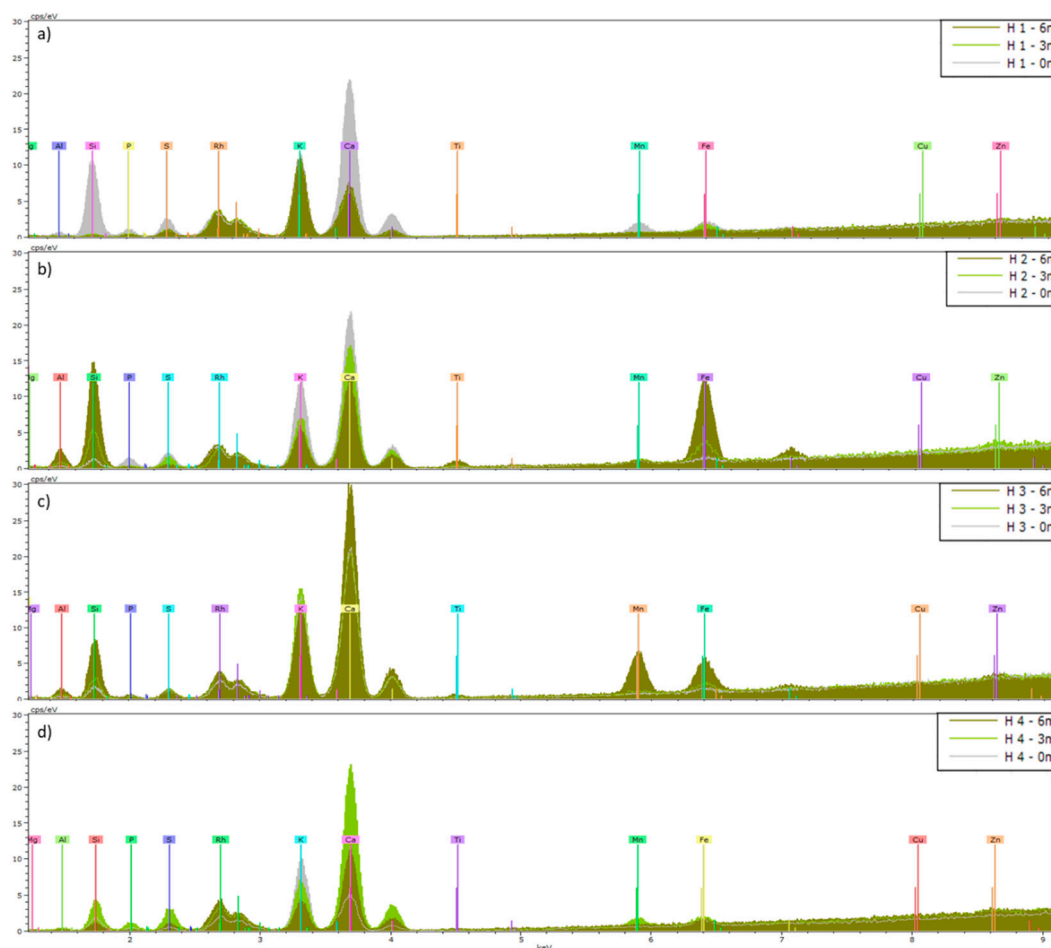


Figure 4. Means (n=5) of XRF spectra of *Hedera helix* (H) leaves collected from a) site 1, b) site 2, c) site 3 and d) site 4. Leaves were analyzed before (0m) and after 3 and 6 months of exposure (3m and 6m). The KeV of the peaks shows which elements are present, and the height of a peak indicates the abundance of that element.

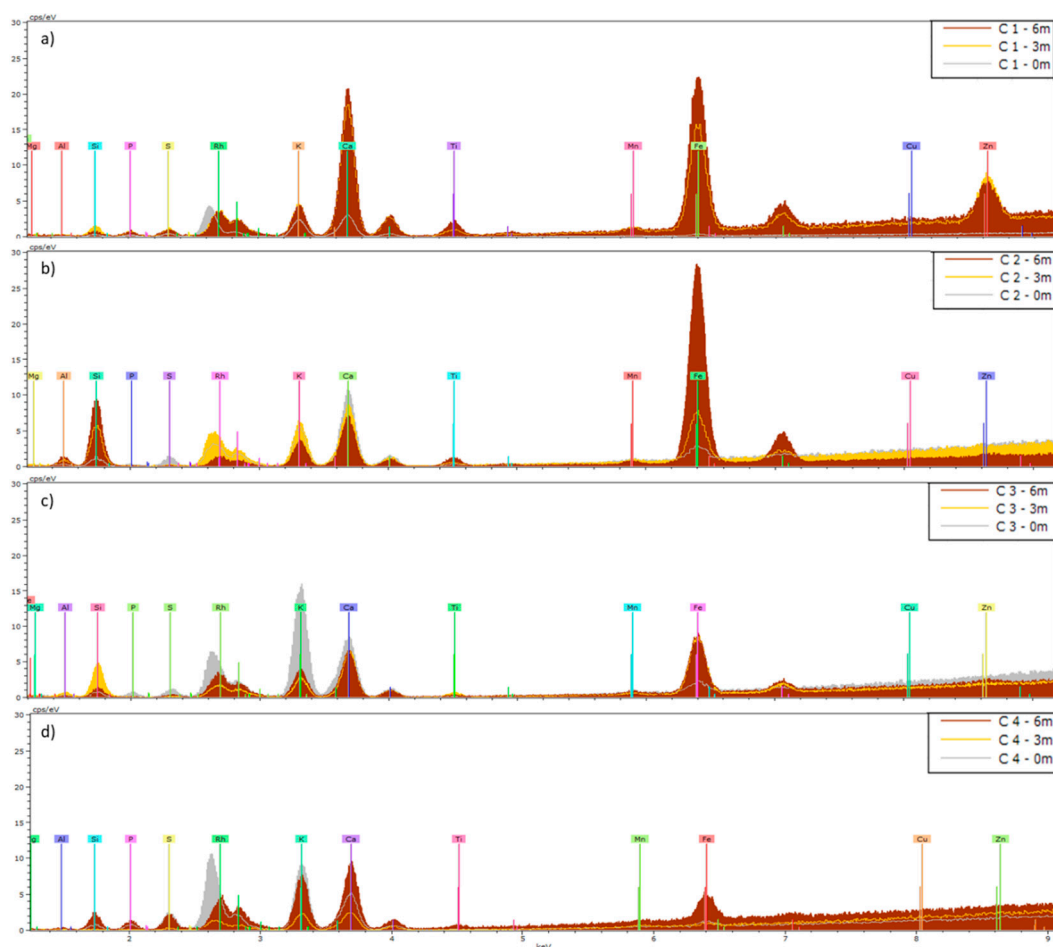


Figure 5. Means (n=5) of XRF spectra of *Senecio cineraria* (C) leaves originating from a) site 1, b) site 2, c) site 3 and d) site 4. Leaves were analyzed before (0m) and after 3 and 6 months of exposure (3m and 6m). The KeV of the peaks shows which elements are present, and the height of a peak indicates the abundance of that element.

Figure 6 shows the mean element concentrations, and standard deviations, of the elements quantified by ICP in *Hedera helix* and *Senecio cineraria* leaves. Moreover, Figure 7 shows the biplot based on the first two principal components, which explain around 99.42% of the variability, of the PCA analysis. Sample distributions were categorized by (A) site and plant species, (B) exposure time in months, while (C) the loading plot emphasizes elements that influence sample distributions. The same elements measured by XRF were detected by ICP, except Ti, Si and Al. Cd was detected by ICP analyses in leaves of *Hedera helix* and *Senecio cineraria* located at sites 1, 2 and 3. The highest accumulation was recorded after 3 months at site 2. Cd was not detected by XRF. Likely, the high K peak in the XRF spectra may overlap with Cd lines, obstructing its detection and quantification in case Cd is present in low concentrations. Also, Cu was only detected by ICP.

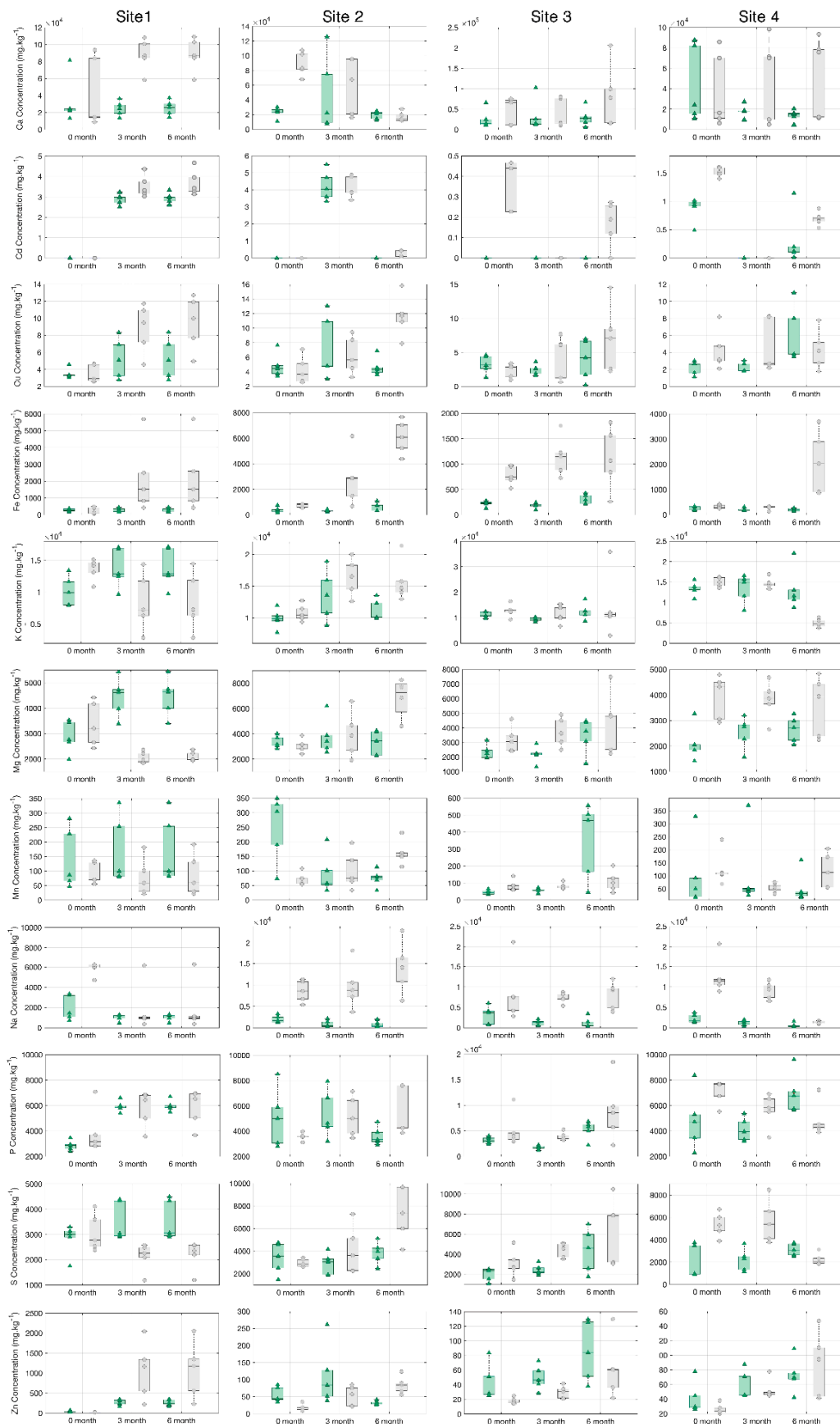


Figure 6. Boxplot mean element concentrations (mg.kg⁻¹) and standard error (n=5) in leaf tissue across sites and months for *Hedera helix* (green triangle) and *Senecio cineraria* (gray circle) by ICP.

Senecio cineraria samples from sites 1 and site 2 are separating from the rest of the samples (Figure 7A). Site 2 shows a dispersion across the PC1 explaining the 96.28% of the total variance and site 1 demonstrates a dispersion across the PC2 explaining the 3.14% of the total variance. Figure 7C suggests a direct influence of Zn in the separation of *Senecio cineraria* located in site 1 across the PC2 and the influence of Fe in the separation of *Senecio cineraria* located in site 2 across the PC1. This indicates that PM-Zn is more typical for high traffic zones (Site 1) and PM-Fe is abundant in unpaved street locations (Site 2). The loading values of Zn and Fe in the two first principal components of PCA explain more than 99.42% of the data variation suggesting that these two elements were the main factors causing the difference in element composition between samples. Furthermore, Cu and Mn displayed an influence in the coordinate origin area, indicating that samples from sites 3 and 4 can be enriched with these elements. Figure 7B shows that samples taken at time points 0 and 3 months have a similar distribution, suggesting a variation in trace elements concentrations after the third month. After 3 months of exposure, leaf trace element concentrations exhibited significant decreases ($p > 0.05$) for Cd, Ca and Na (Table S2) and increases for Zn, Cu and Fe.

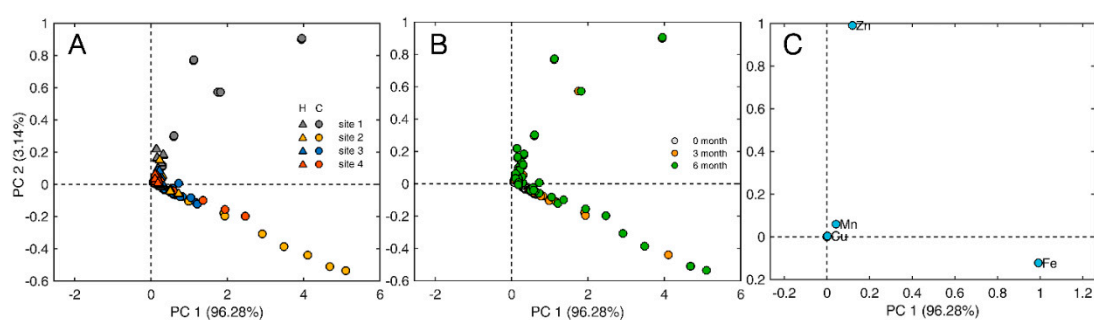


Figure 7. Scores plot of the first two PCs obtained by PCA illustrating sample distributions based on (A) site and plant species ('C' for *Senecio cineraria* and 'H' for *Hedera helix*) and (B) exposure time in months. (C) Loading plot highlighting elements with main influence on the sample distribution.

Welch two sample t-test comparison of a total of nine (common) elements (Ca, Fe, K, Mg, Mn, Na, P, S and Zn) measured by XRF and ICP showed that the average leaf surface elemental concentration of Ca, Fe, Na and Zn were statistically similar ($p > 0.05$) when determined by both techniques for both plant species. P, Mg and S average concentrations were higher when determined by ICP, while, the averages concentrations for K and Mn were always higher after using XRF (Figure 8).

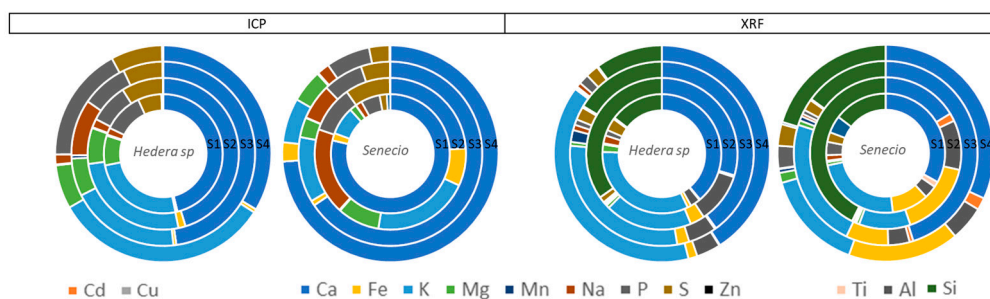


Figure 8. Pie charts of average leaf surface elemental concentration measured by ICP and XRF for *Hedera helix* and *Senecio cineraria* plants after 6 months of exposure at sites 1, 2, 3 and 4. Cd and Cu (left side) were only detected by ICP. Al and Si (right side) were only detected using XRF.

3. Discussion

Meteorological conditions were recorded by Argentina's National Meteorological service, Creative Commons 2.5 Argentina License (Figure 1). According to the climate classification of Thornthwaite, the climate of the center and south of this agricultural zone (Santa Rosa) is dry subhumid, with little or no excess water, cold temperate mesothermal with a summer concentration of thermal efficiency less than 48 % [15]. Temperature, precipitation, humidity and wind speed were related with concentrations recorded by automatic monitors (Figure 2) by Spearman correlation test. It has been reported that a lower temperature leads to a higher humidity, which leads to an increase of both PM_{2.5} and PM₁₀ deposition and absorptions by plants [16]. The effect of air humidity on deposition is due to the fact that particles are mainly hygroscopic, and their size varies as a result of the absorption or discharge of water. In return, this leads to a change in their deposition properties as a function of diameter [17]. Our results showed a positive correlation between temperature and PM₁₀ and PM_{2.5} for sites 3 and 4 and a negative correlation between humidity and PM₁₀ across all sites (Figure 3). Regarding wind speed, Mei et al., [18] reported that an increase in wind speed enhanced particle transport and reduced local particle concentrations, however, it did not affect the relative location of high particle concentration zones, which are more related to building height and design. Agreeing with Mei et al., we just found at site 4 (rural area) a positive correlation between wind speed and PM₁₀ (Figure 3). Additionally, Liu et al. [19] reported that precipitation has a certain wet scavenging effect on PM_{2.5} and PM₁₀, and the scavenging effect on PM₁₀ is higher than that on PM_{2.5}. They concluded that the scavenging effect of precipitation on PM₁₀ is closely related to the initial concentration of PM₁₀ before precipitation. The higher the initial concentration of PM₁₀ is, the greater the removal by precipitation. A negative correlation was observed across all sites between precipitation and PM₁₀, nonmatter the initial concentration of PM₁₀, whereas this correlation was evident only at sites 2 and 3 when considering PM_{2.5} (Figure 3).

Gravimetric quantification of PM deposited on leaves (Table 1) indicates a significant difference in the amounts of PM₁₀ sequester by *Senecio cineraria* in contrast with *Hedera helix*. Deposition was already reported to be mainly affected by the shape of the plant and the structure of the leaves or needles [20]. Also, *Senecio cineraria* leaves are covered with fine matted hairs giving them a felted or woolly appearance [21]. The accumulation of atmospheric PM reported by Castanheiro et al. [22], was shown to be species specific (hedera accumulated more than strawberry) rather than influenced by the buildup of atmospheric dust. Urban, rural, and industrial areas were studied using the leaves of *Celtis occidentalis* and *Trientalis europaea* in the city of Debrecen (Hungary) [11]. In contrast to our findings, an increasing amount of fine dust deposited on leaves was found in the urban area compared to the industrial and rural sites, suggesting that the higher vehicular traffic had a notable effect on dust emission and deposition on leaves at the urban site. Similarly, in the city of Gandhinagar, India, Chaudhary et al. [23] found higher dust depositions on tree leaves in zones with intense traffic compared to commercial and residential zones. However, we did not find additional PM deposition at the urban site (site 1) compared to the peri-urban sites (sites 2 and 3) and the rural site (site 4). This might be due to the fact that in the urban site the diffusion of PM was not hindered by tall rows of buildings. There was not a correlation between the location where plants sequestered the highest amount of PM (site 3, Table 1) and the location where the monitors reported the highest amount of PM (site 2, Figure 1). Outcomes obtained with both techniques (automatic monitors and bio-monitors) are not associating, however they can be used as complementary tools to elucidate the complex, multifactorial process of PM diffusion and deposition. After characterizing the heavy metal concentrations in a total of 540 samples from four ecosystem compartments (plant leaves, foliar dust, surface soil, and subsoil), Li et al. [24] concluded that foliar dust reflected pollution of atmospheric particulate matter in the most reliably ways among the four ecosystem compartments that were investigated.

After 3 and 6 months of exposure, the predominant elements found enriching PM deposited on *Hedera* an *Cineraria* leaves included Ti, Zn and Fe, by XRF (Figure 4 and 5). Some researchers have reported that Fe could be associated with soil resuspension since this element is a typical soil constituent [25]. Zn and Fe can be derived from exhaust and non-exhaust road traffic [26]. Zn is also

associated to tires tread dust [27]. While, Ti is widely used in paints as a UV filter as well as in plastics [28] and has been detected before in outdoor air [29,30]. Similar results were reported by Castanheiro et al. [22]. They studied accumulation of atmospheric dust on leaves of ivy and strawberry using XRF and concluded that XRF offers many advantages for multi-element, non-destructive analysis, which can be performed directly on the sample, at relatively low cost and with rapid output. However, disadvantages are due to the heterogeneity of plant material and matrix effects [22]. Particularly when samples do not meet the condition of thin-film, self-absorption effects arise that complicate the process of matrix calibration required for quantitative analysis [31]. In our study these effects were also observed as the variabilities between leaves from the same species and exposure time were larger than expected (Table S1). Santos et al. [25], used *Nerium oleander* L. leaves as bio-monitor to evaluate levels of environmental pollutants in a sub-region in the Metropolitan Area of Rio de Janeiro City (Brazil) through XRF. In their study they highlighted the association between Fe, Cu, Zn, and Pb and vehicle and industrial emission sources and the usability of the XRF technique for environmental pollution analysis. While, according to Hulskotte et al. [32] vehicle braking system is one of the most important sources of Cu particles. In our study, enrichment of Cd, Cu, Fe, Mn and Zn in leaves was found to result from accumulation of atmospheric dust by ICP (Figure 6).

For the interpretation of field data and evaluation of trace element air pollution, reference values are needed. "Reference Plant" was proposed by Markert [33] and it describes the average content of all the inorganic elements found in plants. The following values could be considered as 'normal' metal concentrations in leaves of plants from uncontaminated environments: 0.05 mg.kg⁻¹ Cd, 10 mg.kg⁻¹ Cu, 150 mg.kg⁻¹ Fe, 200 mg.kg⁻¹ Mn and 50 mg.kg⁻¹ Zn. These values of element concentration can be further used to establish the reference point of the "chemical fingerprint" [34]. In our study, Cd, Fe and Zn exceed these thresholds (Figure 6 and Table S2). These elements may become a threat to human health and/or the environment. Chronic exposure to low levels of heavy metals can cause serious health effects in the long term [35]. Gehring et al. [36] described the adverse effects of PM constituents, in particular Si, K, Fe, Cu and Zn, on asthma, rhinitis, allergic sensitization, and lung function in schoolchildren.

Finally, results obtained by XRF (not destructive) and ICP (destructive) analytical techniques were compared by Welch two sample t-test (Figure 8). Castanheiro et al. [22] also compared results obtained by XRF and HRICP-MS techniques of leaves of ivy and strawberry exposed to atmospheric dust. For a total of ten (common) elements (Si, K, Ca, Ti, Cr, Fe, Cu, Rb, Sr, Pb), they observed that concentrations were always higher when samples were investigated using XRF in comparison with ICP-MS. However, those ten elements were detected for most analysed leaves with ICP-MS, which was not the case for XRF. Therefore, they consider the accumulation of elements to be most accurate after quantification by HR-ICP-MS. In contrast, our study showed that XRF and ICP results were statistically similar for Ca, Fe, Na and Zn. While, Cd and Cu were just detected by ICP due to K peaks overlapping by XRF and Ti, Si and Al were just detected by XRF due to heterogeneity of plant material and low detection limits by ICP.

Although it is necessary to perform more research to elucidate whether these plants species can be used as bio-monitors in areas with higher pollution levels, *Cineraria* features make it a promising candidate to be adopted as a bio-monitor or even for PM mitigation when planted as green belts.

4. Materials and Methods

4.1. Selection of Plant Species

Hedera helix: is an evergreen climbing plant with alternating leaves, 50-100 mm long, with 15-20 mm long petioles. It possesses palmately five-lobed juvenile leaves on creeping, climbing stems and unlobed cordate adult leaves on fertile flowering stems exposed to full sun (Metcalf, 2005). This species was chosen for its known capacity to capture a wide spectrum of PM fractions (0.2-2.5 µm; 2.5-10 µm; 10-100 µm) [37,38].

Senecio cineraria: is a white-wooly, heat and drought tolerant evergreen subshrub. The leaves are pinnate or pinnatifid, 5-15 cm long and 3-7 cm broad, stiff, with oblong and obtuse segments, and like the stems, covered with long, thinly to thickly covered with grey-white to white hairs. The

tomentum is thickest on the underside of the leaves, and can become worn off on the upper side, leaving the top surface glabrous with age [39]. This species was chosen as its capacity to accumulate PM has not yet been evaluated and the characteristics of its leaves make it a good candidate to sequester PM.

4.2. Sites Selected, Air Quality Monitoring Stations and Daily Meteorological Conditions

Hedera helix and *Senecio cineraria* plants were obtained from a plant nursery (Agropecuaria, Santa Rosa, Argentina). After the collection of non-exposed cleaned leaves, five plants of each species were placed at the final locations. Four locations in Santa Rosa, La Pampa, Argentina with different anthropogenic impacts were selected for the study. Site 1: University, urban area with intense car traffic based on Google Maps Traffic statistics (-36.625325 Lat., -64.293103 Long.); Site 2: Calo street, a suburban area with moderate car traffic and unpaved streets (-36.647888 Lat., -64.276939 Long.); Site 3: Felice street, located in a residential area with moderate car traffic (-36.627074 Lat., -64.323317 Long.); Site 4: Agronomic Campus, located 5 km from Santa Rosa city, rural area, with little car traffic (-36.548932 Lat., -64.299345 Long.) (Figure S1). Plants were placed next to an automatic air quality measuring station, equipped with a laser scattering Sensor SDS-011 (Nova Fitness, Shandong, China) (Fig S2). Daily meteorological conditions (temperature, precipitation, humidity and wind speed) were recorded by Argentina's National Meteorological service, Creative Commons 2.5 Argentina License. Plants were watered once a week to prevent drought stress. The watering was performed avoiding any physical contact with the leaves. Leaf sampling was conducted every three months during a period of six months, in the spring (December 15th 2021) and in summer (March 16th 2022). Leaves were sampled at 10 cm above the soil, to avoid direct soil contamination and to standardize any potential influence from resuspension of the soil in the pots. Three leaves per plant were collected per sampling location (n=60).

4.3. Sites Selected, Air Quality Monitoring Stations and Daily Meteorological Conditions

An Erlenmeyer was filled with 50 ml of ultrapure water and one leaf was added. The leaf was stirred in an orbital shaker for 60 min at 270 rpm as described previously [40]. Subsequently, PM fractions were separated using Type 91 Whatman ashless filters with 10 μm retention and Type 42 with 2.5 μm retention. Before use, the filters were dried overnight in an oven at 60 $^{\circ}\text{C}$, and their weight was determined to correct for air humidity. After filtration, filters were dried and post-weighed using a PIONER precision balance (OHAUS, Lindavista, Mexico) to calculate the weight of PM in each fraction of every sample. The leaf surface area was determined using Image J Analysis System [41], which allowed to express the amount of PM as mg cm^{-2} leaf area.

4.4. Leaf Surface Elemental Composition: XRF and ICP

Leaf samples were analyzed for their elemental composition using X-Ray Fluorescence (XRF) and Inductively Coupled Plasma-Atomic Emission Spectrometry (ICP). First, leaf samples were analyzed by XRF for the elements range Na–Ba. An XRF benchtop spectrometer (M4 Tornado, Bruker®, Germany), equipped with a Rh X-ray tube with polycapillary optics and XFlash® detector providing an energy resolution of better than 145 eV was employed. For the analyses of (i) Mg–Fe we used: tube voltage of 10 kV, current of 300 mA, live time of 500 s; and for (ii) Ti–Ba: 40 kV, 50 mA, 1000 s. The measured XRF spectra in each pixel of the XRF maps were deconvoluted using the software supplied with the M4 Tornado. Spectrum energy calibration was performed daily, before the analysis of each batch, by using a copper (Cu) and zirconium (Zr) Bruker® calibration standard block. Analytical quality control was ensured by analysis of steel certified reference material (SN0163). Data was normalized against a conservative element and results were informed in % weight normalized to 100 %.

Secondly, the same leaves were digested with 70% HNO_3 in a heat block and dissolved in 5ml of 2% HCl using the USEPA 3050B Acid Digestion of Sediments, Sludges, and Soils (Environmental Protection Agency [EPA] 1996a). The concentrations of elements were determined by inductively

coupled plasma-atomic emission spectrometry (HR-ICP-OES, Agilent Technologies, 700 series, Belgium). Blanks (only HNO₃) were included. Also, certified reference materials, Cabbage-BCR and Spinach Leaves 1570a were included in each batch. The recoveries obtained were in the range of 40-67% for Cd, 77-90% for Cu, 79-90% for Mn, 61-70% for Pb and 79-91% Zn.

4.5. Statistical Analysis

Data normal distribution was verified with the Shapiro-Wilk test and the homogeneity of variances was confirmed by a Levene test. The differences between samples were tested using analysis of variance (ANOVA) for each variable. When group variances were unequal, the Games-Howell method was used for pairwise comparison between the groups. Two-sample t-test was applied to analyze months and species categories. Statistical analysis to compare possible significant differences between XRF and ICP techniques was carried out by the Welch T-test. Principal component analysis (PCA) was carried out to identify the potential contributions of Cd, Cu, Fe, Mn, and Zn and exposure time (0, 3 and 6 months) at each site. Additionally, Spearman correlation analysis was performed to assess correlations between meteorological variables (temperature, wind speed, humidity, and precipitation) and PM fractions (10 and 2.5) at each site. PCA was displayed by Matlab (The MathWorks Inc., Natick, MA), while the correlation matrix was generated using R (version 4.2.2).

5. Conclusions

Hedera helix and *Senecio cineraria* plants were exposed at locations with different road traffic intensities for a period of six months. Plants were placed near air quality monitoring stations. Leaves collected after 0, 3 and 6 months were examined for their elemental and PM contents. Outcomes obtained with automatic monitors and bio-monitors are not associating, however they can be used as complementary tools to elucidate the complex, multifactorial process of PM diffusion and deposition. The accumulation of atmospheric PM was shown to be species specific rather than influenced by the traffic intensity and the atmospheric dust levels Humidity was the climatic variable that was strongly negatively influencing PM recorded by monitors. The unpaved street at site 2 was the only location where PM₁₀ and PM_{2.5} exceeded WHO guidelines. The rugged and matted hairs at its leaf surface make *Senecio cineraria* sequester significantly higher amounts of PM₁₀ and PM_{2.5}. At the high traffic site 1, Zn enriched the PM sequestered by plant leaves and Fe was observed on plants leaves located close to unpaved streets. Furthermore, using XRF, Ti was identified on plants leaves, probably originating from construction activities. XRF and ICP results were statistically similar for Ca, Fe, Na and Zn. However, Cd and Cu were just detected by ICP due to K peaks overlapping by XRF and Ti, Si and Al were just detected by XRF due to heterogeneity of plant material and low detection limits by ICP. Therefore, the two techniques have complementary weaknesses. Based on our results, *Senecio cineraria* may be considered as a bio-monitor or even as part of a PM mitigation strategy.

Supplementary Materials: The following supporting information can be downloaded at: Preprints.org, Figure S1: Sample sites locations in Santa Rosa City, La Pampa province, Argentina. a) Site 1, urban area with high car traffic; b) Site 2, suburban area with moderate car traffic and unpaved street; c) Site 3, residential area with moderate car traffic; d) Site 4, rural area with low car traffic, based on Google Maps Traffic; Figure S2: Particulate matter monitoring station. a) Operative monitoring station; b) Inside monitoring station; c) Detail of matriculate matter sensor (Nova fitness SDS011); Figure S3: Image acquired by XRF camera applying background correction and reduced image range. a) *Hedera helix*; b) *Senecio cineraria*; Figure S4: Daily average concentrations of PM₁₀ and PM_{2.5} recorded at each site. Pink line represents the WHO annual threshold (PM₁₀= 15 µg m⁻³; PM_{2.5}= 5 µg m⁻³); Table S1: Semi quantitative element concentrations Normalized wt % in leave tissue of *Hedera helix* and *Senecio cineraria* by XRF; Table S2: Element concentrations (mg.kg⁻¹) in leave tissue of *Hedera helix* and *Senecio cineraria* by ICP.

Author Contributions: Data curation, formal analysis, writing original draft, Anabel Saran; Methodology and supervision, Mariano Mendez; Software, Diego Much; Review and editing, Valeria Imperato; Conceptualization and supervision, Sofie Thijs; Conceptualization, supervision, review and editing, Jaco Vangronsveld;

Conceptualization, project administration, resources, supervision, review and editing, Luciano Merini. All authors have read and agreed to the published version of the manuscript.

Funding: This research was supported by the Pluriannual Projects of Investigation-CONICET, grant number PIP-0730 and the Centre for Environmental Sciences, Hasselt University, Belgium, under grant BOF-BILA N°8546.

Conflicts of Interest: The authors declare no conflicts of interest. The funders had no role in the design of the study; in the collection, analyses, or interpretation of data; in the writing of the manuscript; or in the decision to publish the results.

References

1. EEA Air Quality in Europe-2017 Report. **2017**, doi:10.2800/850018.
2. WHO WHO Global Air Quality Guidelines: Particulate Matter (PM_{2.5} and PM₁₀), Ozone, Nitrogen Dioxide, Sulfur Dioxide and Carbon Monoxide: Executive Summary.
3. Oliva, S.R.; Espinosa, A.J.F. Monitoring of Heavy Metals in Topsoils, Atmospheric Particles and Plant Leaves to Identify Possible Contamination Sources. *Microchemical Journal* **2007**, *86*, 131–139, doi:10.1016/j.microc.2007.01.003.
4. Ioannidou, E.; Papagiannis, S.; Manousakas, M.I.; Betsou, C.; Eleftheriadis, K.; Paatero, J.; Papadopoulou, L.; Ioannidou, A. Trace Elements Concentrations in Urban Air in Helsinki, Finland during a 44-Year Period. *Atmosphere (Basel)* **2023**, *14*, doi:10.3390/atmos14091430.
5. J. Luo; H. Liu; S. Hua; and L. Song Retracted: The Correlation of PM_{2.5} Exposure with Acute Attack and Steroid Sensitivity in Asthma. *Biomed Res Int* **2024**, *2024*, 9891074.
6. Li, R.; Zhou, R.; Zhang, J. Function of PM_{2.5} in the Pathogenesis of Lung Cancer and Chronic Airway Inflammatory Diseases. *Oncol Lett* **2018**, *15*, 7506–7514.
7. Zhao, J.; Li, M.; Wang, Z.; Chen, J.; Zhao, J.; Xu, Y.; Wei, X.; Wang, J.; Xie, J. Role of PM_{2.5} in the Development and Progression of COPD and Its Mechanisms. *Respir Res* **2019**, *20*, doi:10.1186/s12931-019-1081-3.
8. Hantrakool, S.; Kumfu, S.; Chattipakorn, S.C.; Chattipakorn, N. Effects of Particulate Matter on Inflammation and Thrombosis: Past Evidence for Future Prevention. *Int J Environ Res Public Health* **2022**, *19*.
9. Yi, W.Y.; Lo, K.M.; Mak, T.; Leung, K.S.; Leung, Y.; Meng, M.L. A Survey of Wireless Sensor Network Based Air Pollution Monitoring Systems. *Sensors (Switzerland)* **2015**, *15*, 31392–31427.
10. Cozea, A.; Tanase, G. Green Biomonitoring Systems for Air Pollution †. *Engineering Proceedings* **2022**, *19*, doi:10.3390/ECP2022-12654.
11. Molnár, V.É.; Tőzsér, D.; Szabó, S.; Tóthmérész, B.; Simon, E. Use of Leaves as Bioindicator to Assess Air Pollution Based on Composite Proxy Measure (Apti), Dust Amount and Elemental Concentration of Metals. *Plants* **2020**, *9*, 1–11, doi:10.3390/plants9121743.
12. Agarwal, P.; Sarkar, M.; Chakraborty, B.; Banerjee, T. Phytoremediation of Air Pollutants: Prospects and Challenges. *Phytomanagement of Polluted Sites: Market Opportunities in Sustainable Phytoremediation* **2019**, 221–241, doi:10.1016/B978-0-12-813912-7.00007-7.
13. Gupta, G.P.; Kumar, B.; Kulshrestha, U.C. Impact and Pollution Indices of Urban Dust on Selected Plant Species for Green Belt Development: Mitigation of the Air Pollution in NCR Delhi, India. *Arabian Journal of Geosciences* **2016**, *9*, 1–15, doi:10.1007/s12517-015-2226-4.
14. Chen, L.; Liu, C.; Zhang, L.; Zou, R.; Zhang, Z. Variation in Tree Species Ability to Capture and Retain Airborne Fine Particulate Matter (PM_{2.5}). *Sci Rep* **2017**, *7*, doi:10.1038/s41598-017-03360-1.
15. Méndez, M.; Vergara, G.; Casagrande, G.; Bongianino, S. Climate Classification of the Agricultural Region of La Pampa Province, Argentina. *Semiárida Revista de la Facultad de Agronomía UNLPam* **2021**, *31*, 9–20, doi:10.19137/semiarida.2021(02).09-20.
16. Nguyen, T.; Yu, X.; Zhang, Z.; Liu, M.; Liu, X. Relationship between Types of Urban Forest and PM_{2.5} Capture at Three Growth Stages of Leaves. *Journal of Environmental Sciences* **2015**, *27*, 33–41, doi:10.1016/J.JES.2014.04.019.
17. Winkler, P. The Growth of Atmospheric Aerosol Particles with Relative Humidity. *Phys Scr* **1988**, *37*, 223, doi:10.1088/0031-8949/37/2/008.

18. Mei, D.; Wen, M.; Xu, X.; Zhu, Y.; Xing, F. The Influence of Wind Speed on Airflow and Fine Particle Transport within Different Building Layouts of an Industrial City. *J Air Waste Manage Assoc* **2018**, *68*, 1038–1050, doi:10.1080/10962247.2018.1465487.
19. Liu, Z.; Shen, L.; Yan, C.; Du, J.; Li, Y.; Zhao, H. Analysis of the Influence of Precipitation and Wind on PM_{2.5} and PM₁₀ in the Atmosphere. *Advances in Meteorology* **2020**, *2020*, 5039613, doi:10.1155/2020/5039613.
20. Litschike, T.; Kuttler, W. On the Reduction of Urban Particle Concentration by Vegetation - A Review. In *Proceedings of the Meteorologische Zeitschrift*; 2008; Vol. 17, pp. 229–240.
21. Srivastava, N. and B.G. Influence of Micronutrient Availability on Biomass Production in *Cineraria Maritima*. *Indian J Pharm Sci* **2006**, *68*.
22. Castanheiro, A.; Hofman, J.; Nuyts, G.; Joosen, S.; Spassov, S.; Blust, R.; Lenaerts, S.; De Wael, K.; Samson, R. Leaf Accumulation of Atmospheric Dust: Biomagnetic, Morphological and Elemental Evaluation Using SEM, ED-XRF and HR-ICP-MS. *Atmos Environ* **2020**, *221*, 117082, doi:10.1016/J.ATMOSENV.2019.117082.
23. Chaudhary, I.J.; Rathore, D. Suspended Particulate Matter Deposition and Its Impact on Urban Trees. *Atmos Pollut Res* **2018**, *9*, 1072–1082, doi:10.1016/J.APR.2018.04.006.
24. Li, C.; Du, D.; Gan, Y.; Ji, S.; Wang, L.; Chang, M.; Liu, J. Foliar Dust as a Reliable Environmental Monitor of Heavy Metal Pollution in Comparison to Plant Leaves and Soil in Urban Areas. *Chemosphere* **2022**, *287*, 132341, doi:10.1016/J.CHEMOSPHERE.2021.132341.
25. Santos, R.S.; Sanches, F.A.C.R.A.; Leitão, R.G.; Leitão, C.C.G.; Oliveira, D.F.; Anjos, M.J.; Assis, J.T. Multielemental Analysis in Nerium Oleander L. Leaves as a Way of Assessing the Levels of Urban Air Pollution by Heavy Metals. *Applied Radiation and Isotopes* **2019**, *152*, 18–24, doi:10.1016/J.APRADISO.2019.06.020.
26. Amato, F.; Pandolfi, M.; Moreno, T.; Furger, M.; Pey, J.; Alastuey, A.; Bukowiecki, N.; Prevot, A.S.H.; Baltensperger, U.; Querol, X. Sources and Variability of Inhalable Road Dust Particles in Three European Cities. *Atmos Environ* **2011**, *45*, 6777–6787, doi:10.1016/J.ATMOSENV.2011.06.003.
27. Adachi, K.; Tainosho, Y. Characterization of Heavy Metal Particles Embedded in Tire Dust. *Environ Int* **2004**, *30*, 1009–1017, doi:10.1016/J.ENVINT.2004.04.004.
28. Shi, H.; Magaye, R.; Castranova, V.; Zhao, J. *Titanium Dioxide Nanoparticles: A Review of Current Toxicological Data*; 2013;
29. Wu, S.; Deng, F.; Wei, H.; Huang, J.; Wang, H.; Shima, M.; Wang, X.; Qin, Y.; Zheng, C.; Hao, Y.; et al. Chemical Constituents of Ambient Particulate Air Pollution and Biomarkers of Inflammation, Coagulation and Homocysteine in Healthy Adults: A Prospective Panel Study. *Part Fibre Toxicol* **2012**, *9*, doi:10.1186/1743-8977-9-49.
30. Nayebare, S.R.; Aburizaiza, O.S.; Siddique, A.; Carpenter, D.O.; Hussain, M.; Zeb, J.; Aburizaiza, A.J.; Khwaja, H.A. *Ambient Air Quality in the Holy City of Makkah: A Source Apportionment with 1 Elemental Enrichment Factors (EFs) and Factor Analysis (PMF) 2*; 2018;
31. Bilo, F.; Borgese, L.; Dalipi, R.; Zacco, A.; Federici, S.; Masperi, M.; Leonesio, P.; Bontempi, E.; Depero, L. Elemental Analysis of Tree Leaves by Total Reflection X-Ray Fluorescence: New Approaches for Air Quality Monitoring. *Chemosphere* **2017**, *178*, 504–512, doi:10.1016/J.CHEMOSPHERE.2017.03.090.
32. Hulskotte, J.H.J.; Roskam, G.D.; Denier van der Gon, H.A.C. Elemental Composition of Current Automotive Braking Materials and Derived Air Emission Factors. *Atmos Environ* **2014**, *99*, 436–445, doi:10.1016/J.ATMOSENV.2014.10.007.
33. Markert, B. Establishing of “Reference Plant” for Inorganic Characterization of Different Plant Species by Chemical Fingerprinting. *Water Air Soil Pollut* **1992**, *64*, 533–538, doi:10.1007/BF00483363/METRICS.
34. Karmakar, D.; Padhy, P.K. Air Pollution Tolerance, Anticipated Performance, and Metal Accumulation Indices of Plant Species for Greenbelt Development in Urban Industrial Area. *Chemosphere* **2019**, *237*, 124522, doi:10.1016/J.CHEMOSPHERE.2019.124522.
35. Gunathilaka, P.A.D.H.N.; Ranundeniya, R.M.N.S.; Najim, M.M.M.; Seneviratne, S. A Determination of Air Pollution in Colombo and Kurunegala, Sri Lanka, Using Energy Dispersive X-Ray Fluorescence Spectrometry on *Heterodermia Speciosa*. *Turk J Botany* **2011**, *35*, 439–446, doi:10.3906/bot-1006-15.
36. Gehring, U.; Beelen, R.; Eeftens, M.; Hoek, G.; De Hoogh, K.; De Jongste, J.C.; Keuken, M.; Koppelman, G.H.; Meliefste, K.; Oldenwening, M.; et al. Particulate Matter Composition and Respiratory Health the PIAMA Birth Cohort Study. *Epidemiology* **2015**, *26*, 300–309, doi:10.1097/eDe.0000000000000264.
37. Justyna Mazur Plants as Natural Anti-Dust Filters – Preliminary Research. *Czasopismo Techniczne* **2018**, doi:10.4467/2353737xct.18.045.8340.

38. Redondo-Bermúdez, M. del C.; Gulenc, I.T.; Cameron, R.W.; Inkson, B.J. 'Green Barriers' for Air Pollutant Capture: Leaf Micromorphology as a Mechanism to Explain Plants Capacity to Capture Particulate Matter. *Environmental Pollution* **2021**, *288*, 117809, doi:10.1016/J.ENVPOL.2021.117809.
39. Pelsler, P.B.; Gravendeel, B.; Van Der Meijden, R. Tackling Speciose Genera: Species Composition and Phylogenetic Position of Senecio Sect. Jacobaea (Asteraceae) Based on Plastid and nrDNA Sequences. *Am J Bot* **2002**, *89*, 929–939, doi:10.3732/ajb.89.6.929.
40. Imperato, V.; Kowalkowski, L.; Portillo-Estrada, M.; Gawronski, S.W.; Vangronsveld, J.; Thijs, S. Characterisation of the Carpinus Betulus L. Phyllomicrobiome in Urban and Forest Areas. *Front Microbiol* **2019**, *10*, doi:10.3389/fmicb.2019.01110.
41. Schneider, C.A.; Rasband, W.S.; Eliceiri, K.W. NIH Image to ImageJ: 25 Years of Image Analysis. *Nat Methods* **2012**, *9*, 671–675.

Disclaimer/Publisher's Note: The statements, opinions and data contained in all publications are solely those of the individual author(s) and contributor(s) and not of MDPI and/or the editor(s). MDPI and/or the editor(s) disclaim responsibility for any injury to people or property resulting from any ideas, methods, instructions or products referred to in the content.